ISSN 1811-2382, Polymer Science, Series C, 2018, Vol. 60, Suppl. 1, pp. S95–S105. © Pleiades Publishing, Ltd., 2018.

Association Equilibrium and Gelation in Solutions of Cross-Associating Chains Containing Inactive Fragments[1]

I. Yu. Gotlib[a,*] and A. I. Victorov[a]

[a] *Saint Petersburg State University, St. Petersburg, 199034 Russia*

**e-mail: i.gotlib@spbu.ru*

Received April 11, 2018

Abstract—Solutions of two cross-associating chain molecular species (*n*-chains and *p*-chains) containing both associative ("sticky") and non-associative monomer links have been simulated by molecular dynamics. The inactive monomers increase the stickers' association equilibrium constant due to the excluded volume effect. In a wide concentration range, the equilibrium constant can be approximated as a simple function of the total volume concentration of the inert monomers, the volume effectively excluded by one inert monomer being about the same at different mixture compositions. Characteristics of molecular aggregates formed at pre-gelation and gelation conditions are examined, including effects of local cyclization.

DOI: 10.1134/S1811238218020091

INTRODUCTION

Mixed solutions of cross-associating oligomer or polymer species in a low-molecular solvent (in more complex cases, containing also additional low-molecular and/or ionic components) are quite important as they are able to undergo various phase and structural transitions depending on molecular structure and concentrations of the components. They can form gels when intermolecular association produces infinite aggregates, and properties of those gels (depending particularly on lifetimes and density of the associative bonds) can be regulated by varying the mixture composition and external conditions. When the associative interaction is significantly weaker than "standard" covalent chemical bonding, such a system forms a (reversible) physical gel where bonds between the associative groups are created and destroyed many times on a macroscopic, and even microscopic, time scale. A lot of literature has been published on such systems and their practical applications, e.g. [1–4]. However their behavior on the molecular level remains insufficiently studied. A number of works using molecular dynamics (MD), Monte Carlo (MC) or related simulation methods for modeling macromolecular systems with physical gelation have been published, see e.g. [5–9] and references therein, and also a review by Košovan, Richter, and Holm [3]. To the best of our knowledge, there is no systematic study of typical characteristics of molecular aggregation and gelation specific to mixtures containing two multifunctional macromolecular components with cross-association but without self-association (e.g. polycation–polyanion mixtures).

In [10], a simple molecular thermodynamic model based on the Semenov–Rubinstein theoretical approximation [11] was proposed for solutions of two cross-associating polymers and used to model gelation and phase behavior in such systems. Later, we found from MD simulations [12, 13] that for molecules containing non-associative (inert) monomers along with associative ones, this model needs to be corrected, primarily due to the excluded volume effect that causes the inert chain fragments to increase the association equilibrium constant (calculated from concentrations) in comparison with a system with chains consisting of associative monomers only. We proposed a simple mean field approximation for the dependence of the equilibrium constant on the concentration of inert monomers and tested it for solutions of chain molecules of two sorts one of which contains a significant number of non-associative monomer links.

In the present article, we extend the findings of [13] to mixtures of cross-associating chains where both chain species contain a large number of inert monomers. Then we calculate aggregation characteristics of chains in those mixtures, examining a concentration range where gel transition occurs and particularly discussing effects of local cyclization.

[1] The article is published in the original.

MODEL

A detailed description of the model used in our MD simulations was given in our previous publications [12, 13]. It can be summarized as follows. We simulate two sorts of flexible chain-like molecules, *n*-component (*n*-chains) and *p*-component (*p*-chains) in a simple Lennard-Jones solvent. *n*-Chains consist of two kinds of monomer units, *n*-monomers (N) and *o*-monomers (O); similarly, *p*-chains consist of *p*-monomers (P) and *o*-monomers. A monomer unit is composed of the backbone atom (AN, AP, AO) and the excentric dummy atom (DN, DP, DO). An associative bond can be formed between an *n*-monomer and a *p*-monomer while *o*-monomers are inert. The association is modeled as a strong attraction between DN and DP atoms (*n*- and *p*-stickers). Other pairs of dummy atoms (DN–DN, DP–DP, DO–DP, DO–DN, DO–DO) do not attract and exhibit short-range repulsion that ensures that DN–DP association is univalent. The solvent particles (atoms) are denoted AS. All "site-site" interactions between the atoms are represented by Lennard-Jones or (in the case of dummy atoms repulsion) r^{-12} "repulsive Lennard-Jones" potential truncated and smoothly "switched" to zero at some distance. The parameters are chosen to satisfy the equations $4\varepsilon'\sigma'^{12} = 4\varepsilon\sigma^{12} + 4\varepsilon_R\sigma_R^{12}$ and $4\varepsilon'\sigma'^{6} = 4\varepsilon\sigma^{6}$ where ε, σ are the parameters for Lennard-Jones interactions between AN, AP, AO atoms, ε', σ' are the respective parameters for interactions between AS particles and all non-dummy atom species, and ε_R, σ_R describe the repulsion between non-associative dummy atoms. Thus, at long distances, all monomer units (AN+DN, AP+DP, AO+DO) and AS particles behave as equivalent Lennard-Jones sites; this means that the solvent is approximately athermal and that the effective size of all monomer units and AS particles can be considered the same. Besides the non-bonded "site-site" interactions, the model assumes a harmonic potential for chemical bonds within chains and a harmonic cosine potential for valence angles.

The values of parameters of the model potentials are the same that were used in [12] for flexible N_{10} and PO_8P decamers. Before that, they had been used in a coarse-grained representation of poly(ethyleneglycol) [14]. In our model, the mass of solvent molecules and backbone (non-dummy) atoms is 46 atomic units (equal to the mass of $(CH_3)_2O$ molecule) while the dummy atoms are massless. The model potential of DN–DP attraction causing the associative bonding corresponds to bond geometry and strength matching those typical for hydrogen bonds or other specific non-covalent interactions (the potential well is 24.89 kJ/mol in depth, with the minimum at 0.112 nm).

In the present work, we simulate solutions containing $ON_{61}O$, $O(NO)_{30}NO$, $O(NO_2)_{20}NO$, $O(NO_3)_{15}NO$, or $O_4(NO_8)_6NO_4$ *n*-chains, and $O(PO_3)_{15}PO$, $O(PO_5)_{10}PO$, or $O_4(PO_8)_6PO_4$ *p*-chains (hence, all the chain species are 63-mers where all monomer links capable of association are located in non-terminal positions in the chain). Examples of the chains are shown in Fig. 1. The MD simulation cell (with cubic periodic boundary conditions) contains $N_{solv} = 28340$ solvent particles and 820 *n*- and *p*-chains in some proportion, so that the total number of non-dummy atoms is $N = N_N + N_P + N_O + N_{solv} = 28340 + 63 \times 820 = 80000$ and the solvent molar fraction is $x_{solv} = 28340/80000 = 0.35425$. The simulation temperature is $T = 406$ K (corresponding to the reduced temperature $k_BT / \varepsilon = 1$), the pressure is $p =$ 10 bar. From our previous results [13], we can conclude that at those conditions, the modeled mixtures do not show phase separation, hence averaging over the whole volume of the MD cell gives relevant characteristics of the homogeneous solution.

The MD simulations are performed using Nosé–Hoover thermostat and Martyna–Tuckerman–Tobias–Klein barostat. The simulation time step is 0.001 ps. For each composition, the system is equilibrated for 3 ns, and after that, we perform 2 ns production runs, saving configurations every 0.5 ps.

RESULTS AND DISCUSSION

Association Equilibrium and the Crowding Effect

In the same way as in [12, 13], the "apparent" (concentration) equilibrium constants K_{ass} are calculated:

$$K_{ass} = \frac{(N_{pairs}/V)}{((N_N - N_{pairs})/V)((N_P - N_{pairs})/V)} = \frac{p_N}{(1-p_N)(1-p_P)(N_P/V)} = \frac{p_P}{(1-p_N)(1-p_P)(N_N/V)} = \frac{p_N p_P}{(1-p_N)(1-p_P)(N_{pairs}/V)}, \quad (1)$$

where N_{pairs} is the number of bonded *n*-monomer – *p*-monomer pairs in the MD cell, $p_N = N_{pairs}/N_N$ and $p_P = N_{pairs}/N_P$ are the fractions of bonded *n*-monomers and *p*-monomers, respectively, and V is the cell volume.

The calculated values of K_{ass} for different simulated mixtures are presented in Fig. 2 in $\left(\frac{1}{K_{ass}^{1/2}}, \frac{\varphi_O}{v^*}\right)$ coordinates ($\varphi_O = N_O/N$ is the volume fraction of *o*-monomers, and $v^* = V/N$ is the volume per a non-dummy atom, hence $\varphi_O/v^* = N_O/V$ is the volume content of

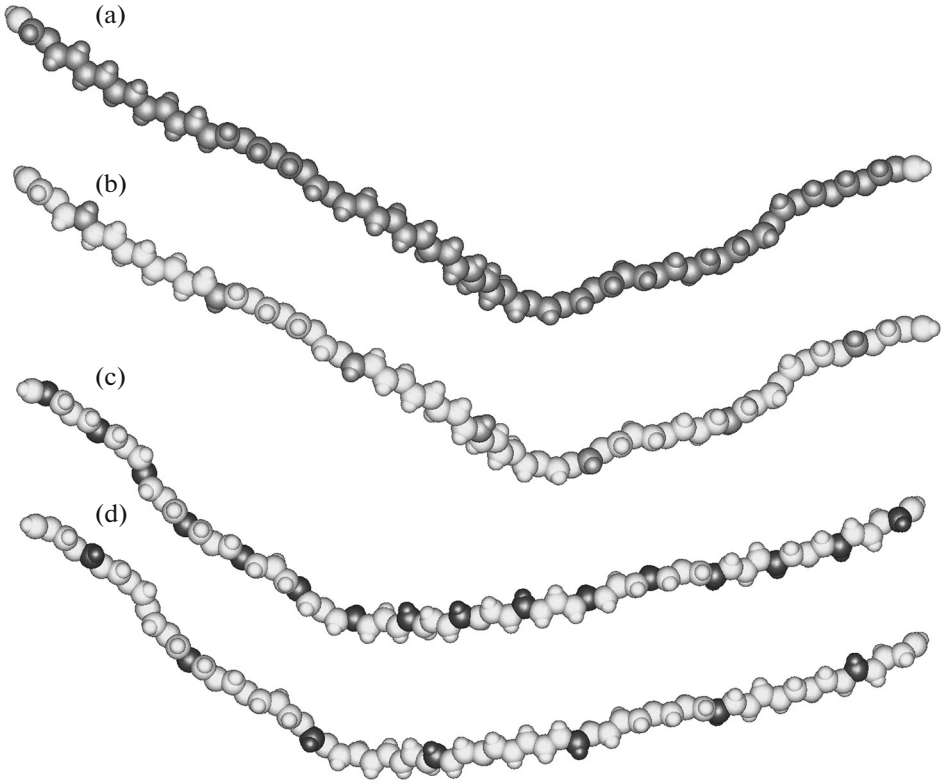

Fig. 1. Examples of *n*- and *p*-chains in the modeled mixtures: (a) $ON_{61}O$, (b) $O_4(NO_8)_6NO_4$, (c) $O(PO_3)_{15}PO$, (d) $O_4(PO_8)_6PO_4$.

o-monomers; reasons for this choice of coordinates were given in [12, 13]). One can see that the approximation proposed in [12, 13],

$$\frac{1}{K_{ass}^{1/2}} = \frac{1}{K_0^{1/2}} - \frac{1}{K_0^{1/2}}\frac{v_0\varphi_O}{v^*}, \qquad (2)$$

holds with a satisfactory accuracy in a wide range of concentrations, except mixtures rich in *p*-component (the component with higher content of *o*-monomers), with the same estimated values of $K_0 = (0.242 \pm 0.003)$ nm^3 and of the effective excluded volume per *o*-monomer, $v_0 = (0.080 \pm 0.001)$ nm^3, for all combinations of *n*- and *p*-components chosen for simulation, independent of the distribution of the inactive monomers between *n*- and *p*-chains. The calculated v_0 is also quite close to the values obtained in [12] for the system containing shorter (decamer) molecules, $N_{10}+PO_8P$ (about 0.082 nm^3 for $x_{solv} = 0.5$). It corresponds to the "effective core diameter" $\sigma_{eff} = (6v_0/\pi)^{1/3} \approx 0.535$ nm $\approx 1.24\sigma' \approx 1.225\sigma'$. The macroscopic volume per a non-dummy atom, v^*, varies between 0.089 and 0.093 nm^3, that is 11–16% higher than v_0, for all the simulated mixtures with $x_{solv} = 0.35425$.

The simple approximation given above is based on an interpretation of the association as a chemical reaction between the two reactant species (non-associated *n*- and *p*- monomers) producing another species (a bonded N–P pair) where the chemical potential of reactants depends on the free volume available for them that decreases due to the presence of inert *o*-monomers, while the chemical potential of the bonded pairs is insensitive to the crowding, e.g. because such pairs are mostly localized in "cages" formed by surrounding monomer units. Another approach is possible, expressed in analytical models like the Semenov–Rubinstein theory [11] and SAFT [15, 16], where the equilibrium constant is presented as a product of factors reflecting energetic, steric ("bonding volume"), and local composition contributions. In our model, the association energetics is fixed, the excluded volume effect from the neighboring inert monomers is included in the steric factor, and the local composition contribution can be separated as a factor g_0 calculated as the average value of the radial distribution function for non-associated N and P monomers within the "reaction sphere" $r \le r_0$ where $r_0 = 0.68$ nm is the maximum observed distance

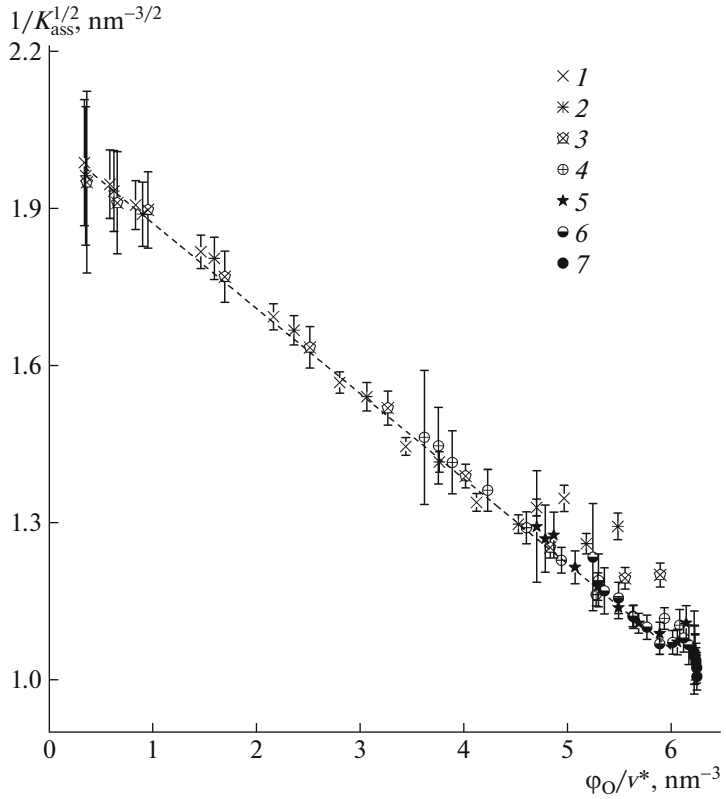

Fig. 2. The concentration equilibrium constant K_{ass} as a function of the volume content of *o*-monomers φ_O/v^* for the simulated mixtures with $x_{solv} = 0.35425$. Error bars represent the mean square fluctuation. The dashed straight line is the fit using Eq. (2), with high-φ_O outliers discarded. (*1*) $ON_{61}O + O(PO_3)_{15}PO$, (*2*) $ON_{61}O + O(PO_5)_{10}PO$, (*3*) $ON_{61}O + O_4(PO_8)_6PO_4$, (*4*) $O(NO)_{30}NO + O_4(PO_8)_6PO_4$, (*5*) $O(NO_2)_{20}NO + O_4(PO_8)_6PO_4$, (*6*) $O(NO_3)_{15}NO + O_4(PO_8)_6PO_4$, (*7*) $O_4(NO_8)_6NO_4 + O_4(PO_8)_6PO_4$. $T = 406$ K.

between *n*- and *p*- monomers in a bonded pair. Figure 3 shows the dependence of g_0 and $(g_0/K_{ass})^{1/2}$ on φ_O/v^*.

One can see that the compositions, where K_{ass} deviates significantly downwards from values predicted by Eq. (2) (hence, $1/K_{ass}^{1/2}$ goes upwards), are those where g_0, after passing through a maximum, decreases with further increase in the concentration of *p*-component. The dependence of $(g_0/K_{ass})^{1/2}$ on φ_O/v^* can be considered as representing the net effect of local chain steric factor as a function of the inert monomers' content. For different mixtures where *n*-component does not contain inactive fragments within the chain ($ON_{61}O + O(PO_3)_{15}PO$, $ON_{61}O + O(PO_5)_{10}PO$, $ON_{61}O + O_4(PO_8)_6PO_4$), these plots are rather close to each other in the whole concentration range. However, they shift to lower $(g_0/K_{ass})^{1/2}$ values (stronger association) when both chain species contain inert "spacers" forming a crowded environment not only around *p*-monomers but around *n*-monomers as well.

Gelation

When bonding between the stickers results in aggregation of associated molecules into an infinite cluster, a (weak physical) gel is formed. Some authors make a distinction between this "geometrical percolation" and "macroscopic gelation" when chain dynamics and mechanical/rheological properties change qualitatively [6]; however, there is another, broader interpretation of physical gelation allowing even water with its network of transient hydrogen bonds to be considered as a weak gel [17].

Predicting quantitatively those concentrations where the percolation transition (gelation, in the broad sense) occurs is not a trivial problem. In the simplest approximation (on which the classical approaches of Flory and Stockmayer are based), the molecules' connectivity graph is described as a Cayley tree. For the system of cross-associating *n*- and *p*-chains, this approximation predicts the gelation threshold at

$$(f-1)p_N(k-1)p_P = 1, \quad (3)$$

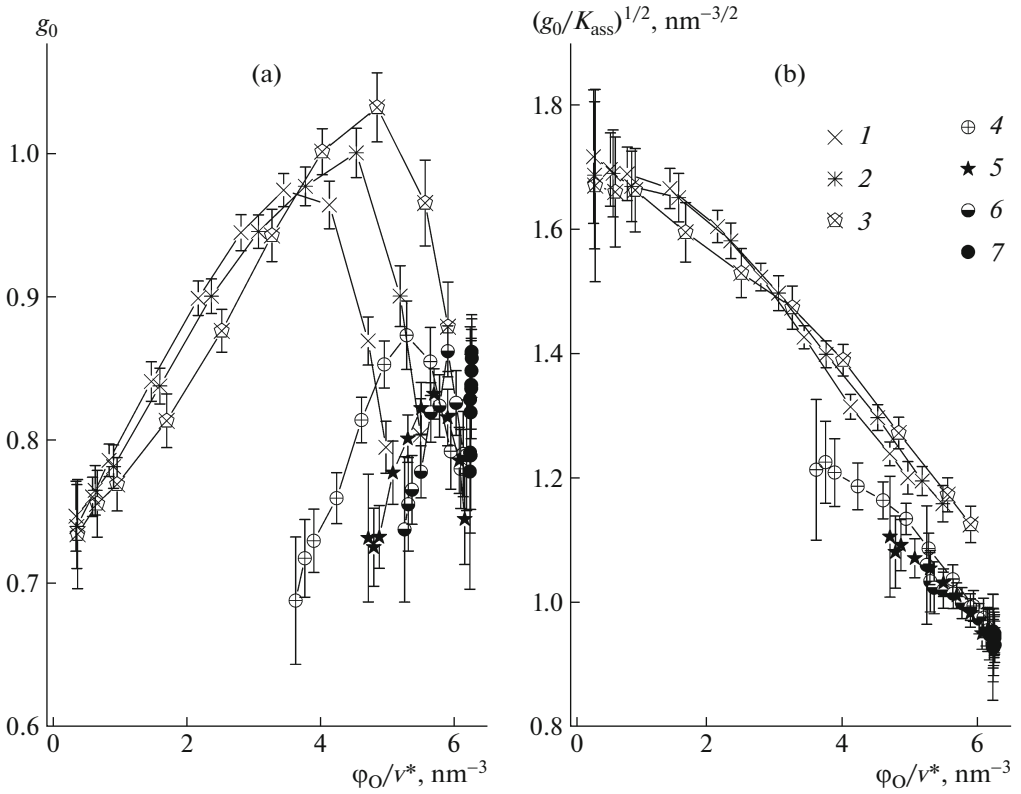

Fig. 3. (a) g_0 and (b) $(g_0/K_{ass})^{1/2}$ as functions of the content of *o*-monomers. (*1*) $ON_{61}O + O(PO_3)_{15}PO$, (*2*) $ON_{61}O + O(PO_5)_{10}PO$, (*3*) $ON_{61}O + O_4(PO_8)_6PO_4$, (*4*) $O(NO)_{30}NO + O_4(PO_8)_6PO_4$, (*5*) $O(NO_2)_{20}NO + O_4(PO_8)_6PO_4$, (*6*) $O(NO_3)_{15}NO+O_4(PO_8)_6PO_4$, (*7*) $O_4(NO_8)_6NO_4 + O_4(PO_8)_6PO_4$.

where f and k are the number of n-stickers per n-molecule and the number of p-stickers per p-molecule, respectively, p_N and p_P are defined above [10]. The average number of molecules in j-th shell of n-chains ("coordination sphere") around a "root" n-chain is

$$S_n = \frac{f}{f-1}\left((f-1)p_N(k-1)p_P\right)^j, \qquad (4)$$

while j-th shell of p-chains around a "root" n-chain contains, on the average,

$$S_p = fp_N\left((f-1)p_N(k-1)p_P\right)^{j-1}, \qquad (5)$$

molecules; hence, $\ln S_n(j)$ and $\ln S_p(j)$ dependences are linear [10, 18]. Actually, however, an infinite Cayley tree (a Bethe lattice) cannot exist in the physical 3-dimensional space, and in a real system with significant aggregation, the molecules' connectivity graph always contains a non-negligible number of loops. As a result of this cyclization, $\ln S_n(j)$ and $\ln S_p(j)$ dependences deviate downwards from linearity, and percolation occurs at higher p_Np_P values than predicted by Eq. (3).

In our simulations, we calculate the connectivity graph for each saved configuration along the MD trajectory and examine clusterization of the chains. With periodic boundary conditions, it is easy to find out whether the system contains an infinite cluster: the necessary and sufficient criterion of its existence is the presence of a molecule that is connected by N–P associative bonds with its own translational image. In Table 1, we present y_{inf}, the proportion of configurations with an infinite cluster among all the configurations saved during the MD run, and $\overline{s}_{fin}$, the average finite cluster size, as well as p_N, p_P, and $(f-1)p_N(k-1)p_P$ at a number of compositions including the percolation region, for $O(NO_3)_{15}NO + O_4(PO_8)_6PO_4$ ($f = 16$, $k = 7$) and $O_4(NO_8)_6NO_4 + O_4(PO_8)_6PO_4$ ($f = 7$, $k = 7$) mixtures. (When calculating $\overline{s}_{fin}$, we do not include isolated chains, that is, those not bonded to any other chain, in averaging because in a cross-associating system without self-association, the stoichiometric excess of one of the components distorts the pattern.) Figure 4 shows the calculated $\ln S_n(j)$ and $\ln S_p(j)$ dependences.

Figure 4 demonstrates the sublinear behavior of $\ln S_n(j)$ and $\ln S_p(j)$ due to formation of loops of asso-

Table 1. The number of n- and p-molecules in the MD cell ($N_n = N_N/f$ and $N_p = N_P/k$), p_N, p_P, $(f-1)p_N(k-1)p_P$, the proportion of configurations with an infinite cluster, y_{inf}, and the average finite cluster size, $\overline{s}_{fin}$, for the model $O(NO_3)_{15}NO + O_4(PO_8)_6PO_4$ and $O_4(NO_8)_6NO_4 + O_4(PO_8)_6PO_4$ mixtures

N_n	N_p	p_N	p_P	$(f-1)p_N(k-1)p_P$	y_{inf}	$\overline{s}_{fin}$
$O(NO_3)_{15}NO + O_4(PO_8)_6PO_4$						
50	770	0.376 ± 0.016	0.056 ± 0.003	2.36 ± 0.20	0.1320	13.53
55	765	0.372 ± 0.018	0.061 ± 0.003	2.54 ± 0.26	0.2467	14.68
60	760	0.374 ± 0.017	0.067 ± 0.004	2.83 ± 0.26	0.4154	14.51
80	740	0.360 ± 0.014	0.089 ± 0.004	3.59 ± 0.28	0.9170	10.07
100	720	0.344 ± 0.011	0.109 ± 0.004	4.20 ± 0.26	0.9950	6.70
620	200	0.068 ± 0.002	0.485 ± 0.013	3.72 ± 0.20	1.0000	4.11
680	140	0.046 ± 0.002	0.507 ± 0.015	2.60 ± 0.16	0.8583	7.15
700	120	0.038 ± 0.002	0.508 ± 0.018	2.17 ± 0.16	0.4806	9.14
710	110	0.035 ± 0.002	0.517 ± 0.018	2.03 ± 0.15	0.3032	9.60
720	100	0.032 ± 0.002	0.526 ± 0.019	1.88 ± 0.14	0.1745	9.46
760	60	0.018 ± 0.001	0.531 ± 0.024	1.09 ± 0.10	0.0039	6.60
$O_4(NO_8)_6NO_4 + O_4(PO_8)_6PO_4$						
100	720	0.373 ± 0.020	0.052 ± 0.003	0.95 ± 0.10	0.0076	5.04
200	620	0.330 ± 0.014	0.106 ± 0.005	1.72 ± 0.14	0.1225	6.43
230	590	0.322 ± 0.012	0.125 ± 0.005	1.98 ± 0.15	0.3349	6.67
250	570	0.312 ± 0.012	0.137 ± 0.005	2.09 ± 0.16	0.4810	6.49
280	540	0.293 ± 0.012	0.152 ± 0.006	2.19 ± 0.17	0.5937	6.18
310	510	0.278 ± 0.011	0.169 ± 0.007	2.31 ± 0.17	0.7304	5.67
410	410	0.229 ± 0.008	0.229 ± 0.008	2.58 ± 0.17	0.9493	4.32

ciated molecules. This effect is relatively weak in solutions far from the percolation threshold (where y_{inf} is zero or close to zero, non-associated molecules and small clusters dominate, and S_n and S_p vanish at some, not very high, j) but becomes quite important in mixtures with higher content of N–P bonds. At compositions close to the gel transition, $\ln S_n(j)$ and $\ln S_p(j)$ have a distinctive shape with inflection. For the system $O(NO_3)_{15}NO + O_4(PO_8)_6PO_4$, we have detected compositions ($N_n = 55$, $N_p = 765$ and $N_n = 710$, $N_p = 110$, with y_{inf} about 0.25–0.3) where S_n and S_p first slightly increase with j, then decrease and then start increasing again. The same compositions are characterized by the highest value of $\overline{s}_{fin}$. This marks an approximate location of the percolation threshold. For the system $O_4(NO_8)_6NO_4 + O_4(PO_8)_6PO_4$, the composition closest to the transition is $N_n = 230$, $N_p = 590$ (or vice versa, as the system is symmetric). Actually, as y_{inf} values show, the gelation transition in the model systems is quite diffuse, and their behavior near the transition is likely strongly influenced by system-size effects.

The inflected shape of $\ln S_n(j)$ and $\ln S_p(j)$ in the gel transition region allows to suggest that the transition occurs when already existing compact clusters start forming interconnections, to produce a large-scale network. This suggests inhomogeneity of the spatial distribution of bonds in systems with strong local cyclization tendencies, as was discussed previously in literature [19, 20]. The dependence of the average gyration radius r_g of a finite cluster on the number of chains in it, s, shown in Fig. 5, confirms the compactness of molecular aggregates: r_g is approximately proportional to $s^{1/3}$ in all simulated mixtures

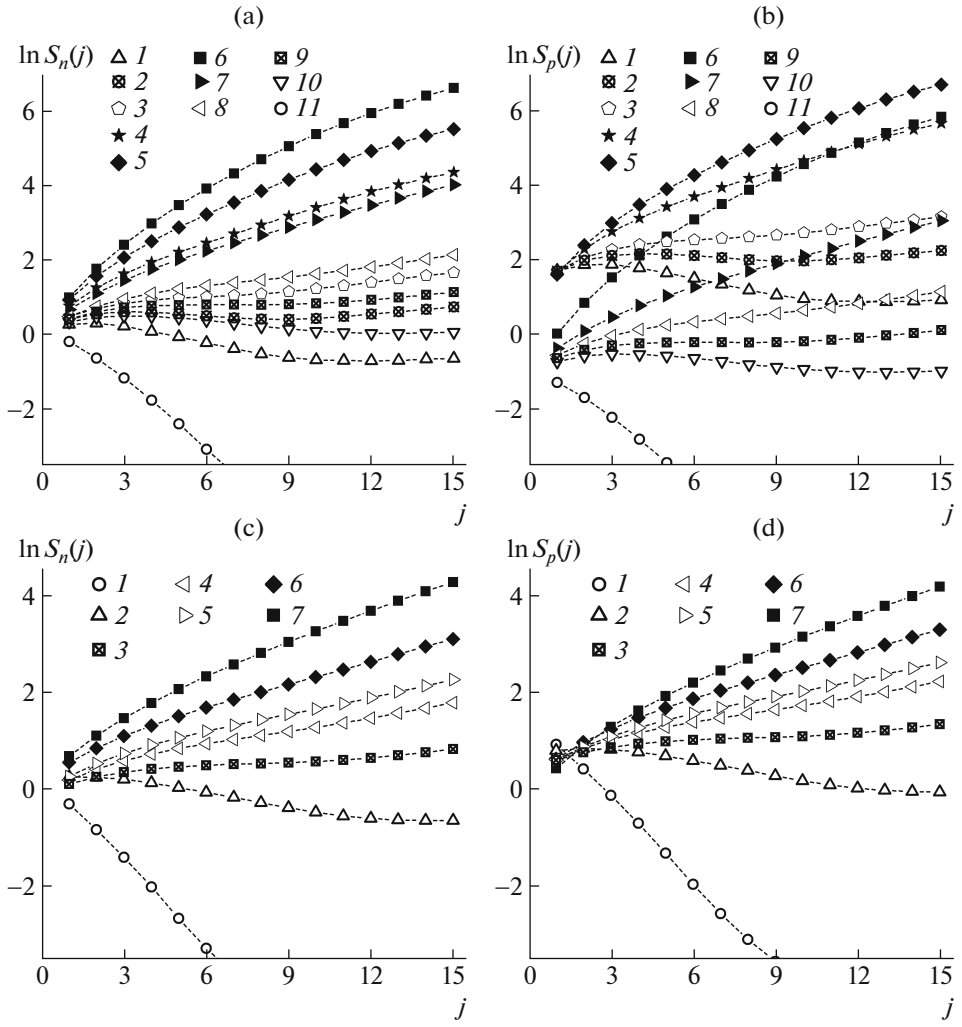

Fig. 4. (a, c) $\ln S_n(j)$ and (b, d) $\ln S_p(j)$ dependences for the model (a, b) $O(NO_3)_{15}NO + O_4(PO_8)_6PO_4$ and (c, d) $O_4(NO_8)_6NO_4 + O_4(PO_8)_6PO_4$ mixtures. (a, b) (*1*) $N_n = 50$, $N_p = 770$, (*2*) $N_n = 55$, $N_p = 765$, (*3*) $N_n = 60$, $N_p = 760$, (*4*) $N_n = 80$, $N_p = 740$, (*5*) $N_n = 100$, $N_p = 720$, (*6*) $N_n = 620$, $N_p = 200$, (*7*) $N_n = 680$, $N_p = 140$, (*8*) $N_n = 700$, $N_p = 120$, (*9*) $N_n = 710$, $N_p = 110$, (*10*) $N_n = 720$, $N_p = 100$, (*11*) $N_n = 760$, $N_p = 60$; (c, d) (*1*) $N_n = 100$, $N_p = 720$, (*2*) $N_n = 200$, $N_p = 620$, (*3*) $N_n = 230$, $N_p = 590$, (*4*) $N_n = 250$, $N_p = 570$, (*5*) $N_n = 280$, $N_p = 540$, (*6*) $N_n = 310$, $N_p = 510$, (*7*) $N_n = 410$, $N_p = 410$.

except for those with the lowest concentration of bonded pairs (and no gelation tendencies). One can expect such a behavior (the cluster fractal dimension close to 3) for a concentrated homogeneous solution (while the different pattern in mixtures poor in associated N–P pairs, especially $O_4(NO_8)_6NO_4 + O_4(PO_8)_6PO_4$ with $N_n = 800$, $N_p = 20$, where small clusters are denser, and large ones, looser, can be attributed to high relative fluctuations of local concentration not only of the associated pairs but of the stoichiometrically deficient component as well).

Table 1 shows that at the transition, $(f - 1)p_N(k-1)p_P$ is significantly higher than 1, especially for mixtures containing chains with more dense arrangement of stickers that is more favorable for local cyclization.

Figure 6 presents the fractions (in proportion to N_n and N_p) of *n*- and *p*-chains participating in small local loops schematically shown in the same figure: 2-loops ($\beta_n^{(2)}$, $\beta_p^{(2)}$), 4-loops ($\beta_n^{(4)}$, $\beta_p^{(4)}$—counting only those chains that are not parts of 2-loops), and 6-loops ($\beta_n^{(6)}$, $\beta_p^{(6)}$—counting only those chains that are not parts of 2-loops or 4-loops). 2-Loops (formed by two chains attached to each other by more than one bond) clearly prevail over larger cycles. While in $O_4(NO_8)_6NO_4 + O_4(PO_8)_6PO_4$ mixtures, no more than 10–11% of molecules are part of the small loops, in $O(NO_3)_{15}NO + O_4(PO_8)_6PO_4$, the total fraction of such chains reaches 60% for *n*-chains and 44% for *p*-chains. This fraction

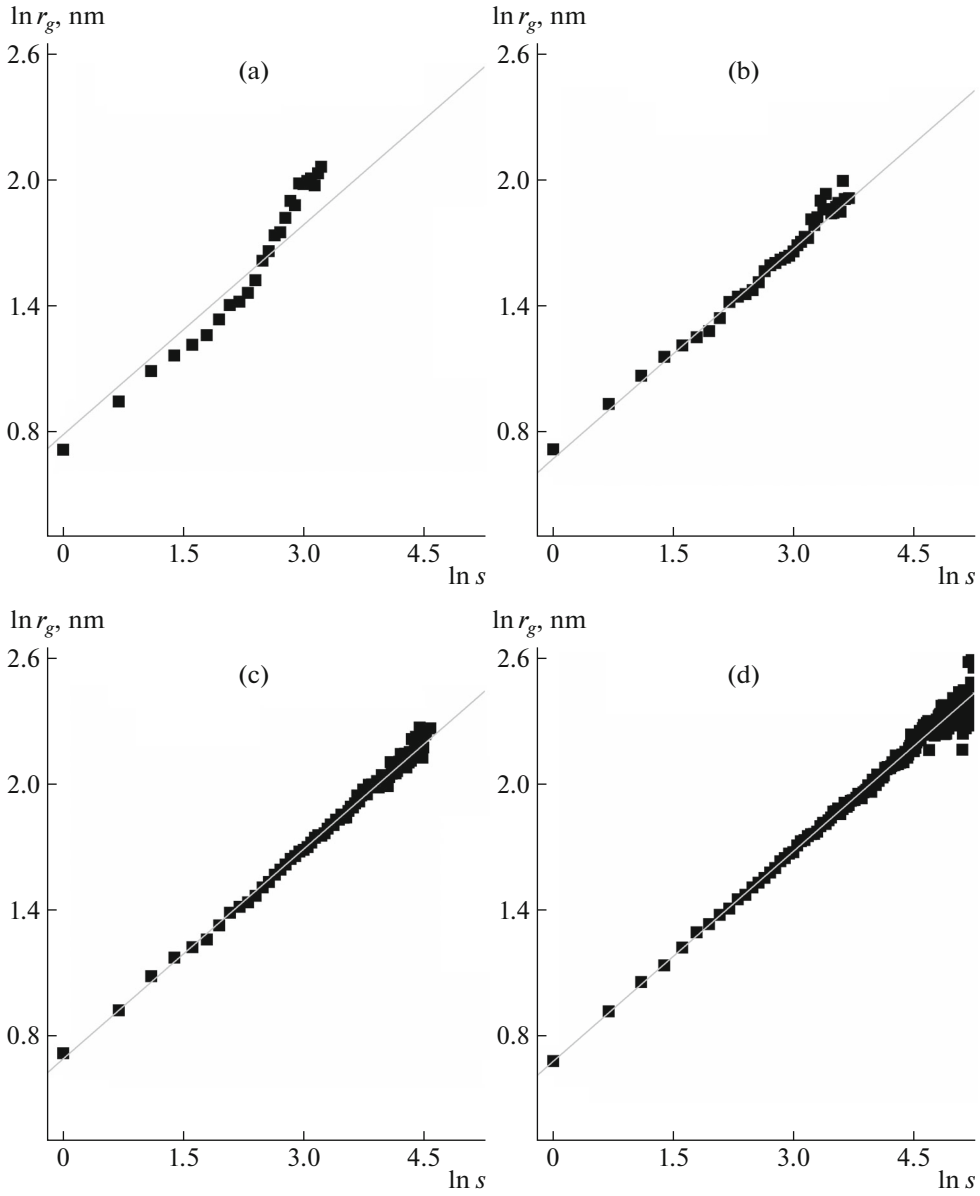

Fig. 5. $\ln r_g(\ln s)$dependence for some simulated mixtures at pre-gel compositions. The straight lines correspond to $r_g \propto s^{1/3}$. (a) $O_4(NO_8)_6NO_4 + O_4(PO_8)_6PO_4$, $N_n = 800$, $N_p = 20$, (b) $ON_{61}O + O_4(PO_8)_6PO_4$, $N_n = 800$, $N_p = 20$, (c) $O(NO_3)_{15}NO + O_4(PO_8)_6PO_4$, $N_n = 760$, $N_p = 60$, (d) $O_4(NO_8)_6NO_4 + O_4(PO_8)_6PO_4$, $N_n = 620$, $N_p = 200$.

is still higher in solutions when at least one component contains a larger number of stickers per chain.

Figure 7 shows the composition dependence of λ_2, the ratio of the number of independent 2-loops in the system to the total number of non-isolated *n*- and *p*-chains, for $O(NO_3)_{15}NO + O_4(PO_8)_6PO_4$ and $O_4(NO_8)_6NO_4 + O_4(PO_8)_6PO_4$ solutions. One can suggest that at gel transition and closely post-transition compositions, there is a slowdown or even a short interruption in the increase of λ_2 with increasing concentration of the stoichiometrically deficient component. This corresponds to the assumption that small cycles are partly being broken when the infinite molecular network is formed (cf. Monte Carlo simulations of a different cross-associating system—a telechelic chain plus a trifunctional junction—in [21]).

The significant presence of small cycles in clusters formed by chains containing many associative sites means that not only the classic approaches of Flory and Stockmayer [22] but also the approximations developed by Erukhimovich, Tamm et al. assuming mesoscopic cyclization [23–25] do not give a good quantitative description of gelation characteristics.

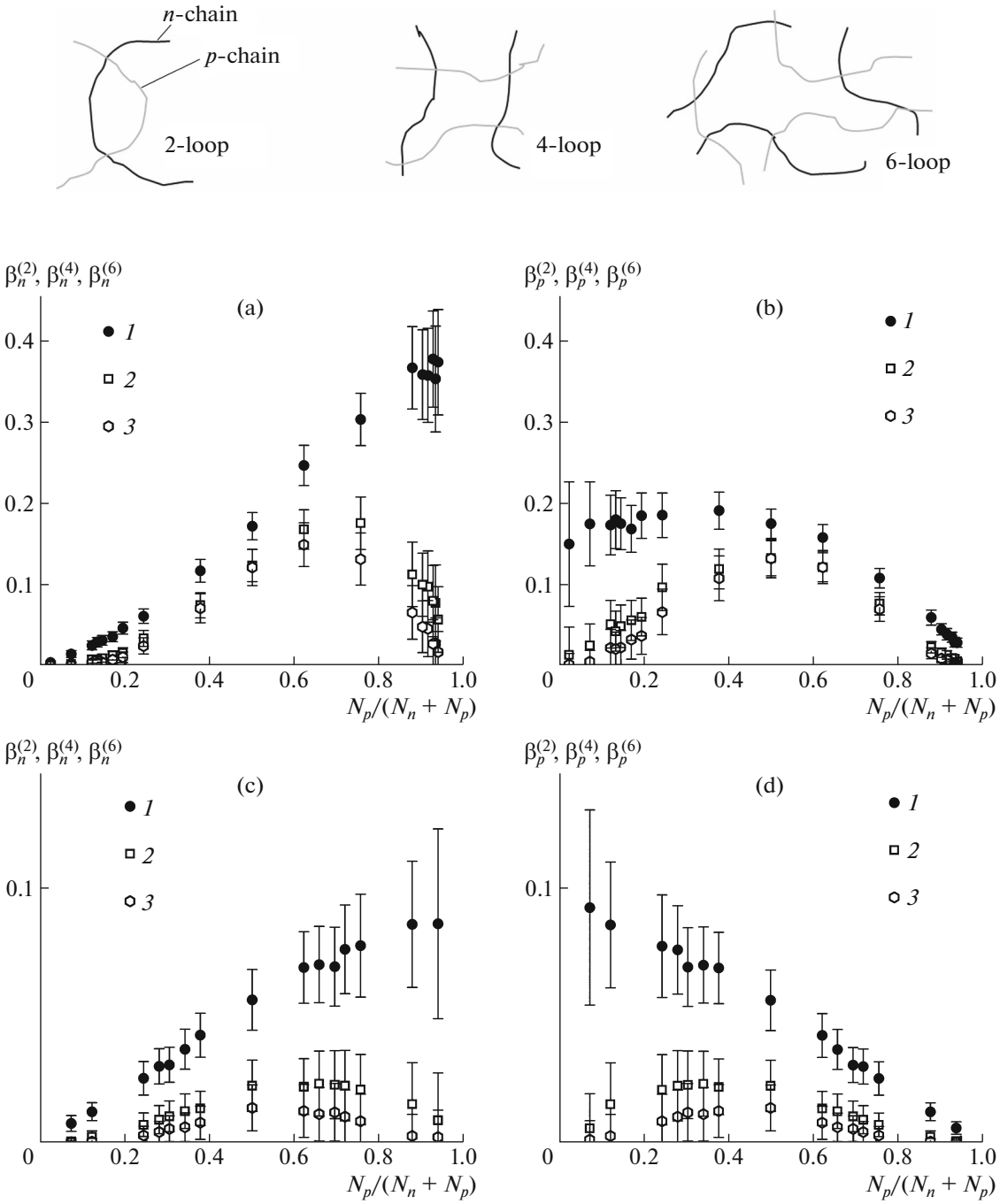

Fig. 6. The fractions of (a, c) *n*- and (b, d) *p*-chains that are part of (*1*) 2-loops, (*2*) 4-loops, and (*3*) 6-loops in the model (a, b) $O(NO_3)_{15}NO + O_4(PO_8)_6PO_4$ and (c, d) $O_4(NO_8)_6NO_4 + O_4(PO_8)_6PO_4$ mixtures.

Indeed, according to [23, 26], the rough criterion of insignificance of corrections due to small loops for a system containing one kind of associating molecules is $(\rho a^3)^{-1} \ll 1$ where ρ is the density of stickers and a is the average distance between neighboring stickers in one molecule. Among our model systems with cross-association, the one with the lowest content of small cycles, the symmetric $O_4(NO_8)_6NO_4 + O_4(PO_8)_6PO_4$ mixture, has $N_N/V = N_P/V \approx 0.39$ nm^{-3} and $a \approx 1.86$ nm, hence $\left(\frac{N_N + N_P}{V} a^3\right)^{-1} \approx 0.2$—not an insignificant value. Attempts to develop an analytical theory describing the delay of gel transition due to small loops' formation were made earlier (see e.g. [27, 28]). However, even more recent advanced models [21] fall

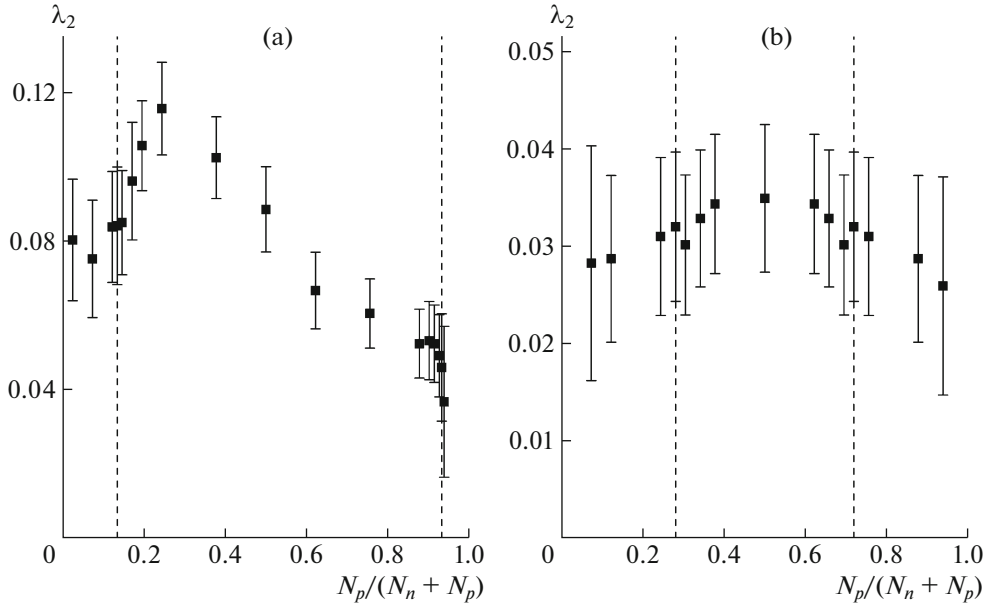

Fig. 7. The number of independent 2-loops as a fraction of the total number of non-isolated *n*- and *p*-chains in the model (a) $O(NO_3)_{15}NO + O_4(PO_8)_6PO_4$ and (b) $O_4(NO_8)_6NO_4 + O_4(PO_8)_6PO_4$ mixtures. The dashed lines show the approximate location of gel transition.

short of a quantitative description of clustering of molecules with many associative sites (particularly, in our simulations, we do not observe a clear relationship between the numbers of 2-loops and larger cycles as the results presented in [21] would suggest).

CONCLUSIONS

Our results allow us to conclude that in binary mixtures of cross-associating chains with inert fragments, where the inert monomers act as crowders, the composition dependence of the "apparent" equilibrium constant of association can be interpreted as an excluded volume effect expressed both through local composition change (*p*-stickers concentrated around *n*-stickers and vice versa) and through steric restrictions directly produced by neighboring inert monomers. In systems where two chain components with different proportions of inactive monomers are mixed, the whole concentration range can be divided into two sub-ranges. As long as the local N–P correlations' measure, g_0, increases with the concentration of the component containing more inert monomer per molecule (*p*-component), K_{ass} depends uniformly on the volume content φ_O/v^* of the inactive monomers, with a constant excluded volume per each inert monomer unit. At higher concentrations of *p*-component, decreasing g_0 leads to lower K_{ass}. The direct local steric effect, as can be seen from the $(g_0/K_{ass})^{1/2}(\varphi_O/v^*)$ dependence, differs for systems where *n*-chains have no inert "spacers" ($ON_{61}O + O(PO_3)_{15}PO$, $ON_{61}O + O(PO_5)_{10}PO$, $ON_{61}O + O_4(PO_8)_6PO_4$) and for those where both *n*-chains and *p*-chains have at least two inert monomers between the stickers ($O(NO_2)_{20}NO + O_4(PO_8)_6PO_4$, $O(NO_3)_{15}NO + O_4(PO_8)_6PO_4$, $O_4(NO_8)_6NO_4 + O_4(PO_8)_6PO_4$), but is almost the same within each of these groups, with the mixture $O(NO)_{30}NO + O_4(PO_8)_6PO_4$ (one inert monomer between the stickers in the *n*-chain) falling in between. This latter difference is not surprising because the closest neighborhood of one sort of stickers (*n*-monomers) differs for the two groups of systems quite significantly, as their neighbors along the chain are other *n*-monomers in the first group, and *o*-monomers in the second group. Thus, a simple mean-field model can satisfactorily describe the effect of inert chain fragments on the association equilibrium as a combination of the two "sub-effects" characterized above.

Our data on the local topology of clusters around gelation transition confirm an important role of small loops, in agreement with the previous findings [21]. For chains of different structure, the value of the left hand side of Eq. (3) at gelation threshold is much greater than the value of the classical criterion and depends on the system composition. Analytical description of this transition still remains among the major challenges for future work.

ACKNOWLEDGMENTS

This work was supported by the Russian Science Foundation (project no. 16-13-10042). The research was carried out using the equipment of the shared

research facilities of HPC computing resources at Lomonosov Moscow State University.

REFERENCES

1. *Polymer Gels and Networks,* Ed. by Y. Osada and A. Khokhlov (Marcel Dekker, New York, 2001).
2. "Gels: Structures, Properties, and Functions. Fundamentals and Applications," Ed. by M. Tokita and K. Nishinari, in *Progress in Colloid and Polymer Science* (Springer, Berlin, Heidelberg, 2009).
3. P. Košovan, T. Richter, and C. Holm, in "Molecular Simulations of Hydrogels, in Intelligent Hydrogels," Ed. by G. Sadowski and W. Richtering, in *Progress in Colloid and Polymer Science,* Ed. by F. Kremer and W. Richtering. (Springer Int. Publ., Berlin; Heidelberg, 2013).
4. "Supramolecular Polymer Networks and Gels," Ed. by S. Seiffert, in *Advances in Polymer Science* (Springer Int. Publ., Heidelberg, 2015).
5. F. A. Escobedo and J. J. de Pablo, Phys. Rep. **318** (3), 85 (1999).
6. S. K. Kumar and J. F. Douglas, Phys. Rev. Lett. **87** (18), 188301 (2001).
7. H. Kobayashi and R. G. Winkler, Sci. Rep. **6**, 19836 (2016).
8. R. G. Pereyra, M. A. Al-Maadeed, and M. A. Carignano, eXPRESS Polym. Lett. **11**, 199 (2017).
9. N. Kamerlin, Doctoral Thesis (Uppsala University, Uppsala, 2017).
10. S. Tcyrulnikov and A. I. Victorov, Macromolecules **46** (11), 4706 (2013).
11. A. N. Semenov and M. Rubinstein, Macromolecules **31** (4), 1373 (1998).
12. I. Y. Gotlib, I. K. Malov, A. I. Victorov, and M. A. Voznesenskiy, J. Phys. Chem. B **120** (29), 7234 (2016).
13. I. Gotlib and A. Victorov, Fluid Phase Equilib. **454**, 116 (2017).
14. H. Lee, A. H. de Vries, S.-J. Marrink, and R. W. Pastor, J. Phys. Chem. B **113** (40), 13186 (2009).
15. W. G. Chapman, K. E. Gubbins, G. Jackson, and M. Radosz, Ind. Eng. Chem. Res. **29** (8),1709 (1990).
16. E. A. Mueller and K. E. Gubbins, Ind. Eng. Chem. Res. **34** (10), 3662 (1995).
17. H. E. Stanley, S. V. Buldyrev, M. Canpolat, M. Meyer, O. Mishima, M. R. Sadr-Lahijany, A. Scala, and F. W. Starr, Phys. A (Amsterdam, Neth.) **257** (1), 213 (1998).
18. K. Emelyanova, I. Yu. Gotlib, A. Shishkina, and A. Victorov, J. Chem. Eng. Data **61** (12), 4013 (2016).
19. S. Seiffert and J. Sprakel, Chem. Soc. Rev. **41** (2), 909 (2012).
20. I. Kryven, J. Duivenvoorden, J. Hermans, and P. D. Iedema, Macromol. Theory Simul. **25** (5), 449 (2016).
21. R. Wang, A. Alexander-Katz, J. A. Johnson, and B. D. Olsen, Phys. Rev. Lett. **116** (18), 188302 (2016).
22. P. J. Flory, *Principles of Polymer Chemistry* (Cornell Univ. Press, Ithaca, N.Y., 1953).
23. I. Erukhimovich, M. V. Thamm, and A. V. Ermoshkin, Macromolecules **34** (16), 5653 (2001).
24. I. Y. Erukhimovich and M. V. Tamm, J. Exp. Theor. Phys. Lett. **75** (3), 150 (2002).
25. M. V. Tamm, PhD Thesis (Moscow State University, Moscow, 2002).
26. S. I. Kuchanov, S. V. Korolev, and S. V. Panyukov, "Graphs in Chemical Physics of Polymers," in *Advances in Chemical Physics,* Ed. by I. Prigogine and S. A. Rice (John Wiley and Sons, Inc., New York, 1988), Vol. 72, pp. 115–326.
27. Z. Ahmad and R. F. T. Stepto, Colloid Polym. Sci. **258** (6), 663 (1980).
28. H. Rolfes and R. F. T. Stepto, Macromol. Symp. **76** (1), 1 (1993).